Fabrication of Suspended Multilevel Three-Dimensional Silicon Micro- and Nano-Structures

S. Azimi* and M. B. H. Breese**

Centre for Ion Beam Applications (CIBA), Department of Physics, National University of Singapore
Singapore 117542
* g0800837@nus.edu.sg
** phymbhb@nus.edu.sg

ABSTRACT

A process for fabricating arbitrary-shaped three-dimensional silicon has been developed, based on high-energy ion irradiation, such as 200 keV to 2 MeV protons and helium followed by electrochemical anodization. This has enabled us to produce suspended complex microstructures such as arrays or long wires, grids, springs, vertically stacked wires and wires which can be controllably bent upwards and downwards in the vertical plane. By using a combination of multiple energy proton irradiation, and gray scale masks, different ion penetration depths and multilevel suspended three-dimensional silicon structures can be obtained in a single etch step.

Keywords: silicon, three-dimensional, suspended, multilevel, arbitrary-shaped, micro- and nano-fabrication

1 INTRODUCTION

Silicon is one of the most attractive materials for many micro- and nanoscale devices, due to its excellent mechanical, optical, and electrical properties. There is a wide spectrum of scientific and technological disciplines in which precisely machined, three-dimensional (3D) micro- and nano-scale structures are required in silicon-based materials. For example, in silicon photonics [1-4] conventional silicon waveguide structures are fabricated in SOI (silicon-on-insulator) wafers, which do not readily allow 3D waveguides between circuitry at different depths within the wafer. Therefore the ability to controllably fabricate 3D lines and wires is highly desirable for coupling between circuits at different depths, and allowing better 3D integration and packing density of photonic devices with each other and with microelectronic components. It would also allow new options for the design and fabrication of high-aspect ratio, multilevel microstructures in silicon for optoelectronic and in micro- and nano-electromechanical systems [5-7] and in fabricating photonic crystals [8].

We have recently developed a technique using ion beam irradiation capable of fabricating arbitrary, curved multilevel 3D structures in bulk silicon in a single etch step [9-10]. In this process, high-energy ions, typically protons or helium, with energies of 200 keV to 2 MeV, are focused to a beam spot of a few hundred nanometers in a nuclear microprobe [11] for direct proton beam writing on p-type silicon. Ion induced defects locally reduce the free carrier density, so increasing the resistivity of the irradiated silicon regions, reducing the rate of porous silicon (PSi) formation during subsequent electrochemical anodization. Higher fluence irradiation can act as an etch stop for PSi formation [12]. The underlying multilevel silicon structure may be easily revealed by removing the PSi with potassium hydroxide (KOH).

2 PRINCIPLES OF 3D SILICON MACHINING USING ION BEAM IRRADIATION

Using ion beam irradiation for silicon machining gives the ability to selectively form PSi inside a bulk silicon wafer, due to the unique characteristic that high-energy protons create significantly more localized defects at their end–of-range than along their penetration path (close to the surface). As an example, Fig. 1 (a) shows SRIM simulation [13] of the trajectories of 1 MeV protons in silicon, which is a typically used energy in this paper for 3D silicon fabrication. The beam tends to remain well-collimated, with little lateral scattering until the ions slow down close to their end-of-range. 1 MeV protons have a range of ~16 µm in silicon, with a FWHM (full-width-at-half-maximum) of the lateral distribution of ~2 µm. The defect generation rate is more than ten times higher at the end of range compared to the trajectory closer to the surface. [14] By controlling the fluence within each point of an irradiated area, the resistivity can be controlled and increased locally for selective PSi formation [14], as shown in Fig. 1 (b). If the fluence is high, during the electrochemical process the flow of electrical holes from the back surface bends around the high defect regions to the front surface. As a result PSi forms around these regions, leaving the core region intact, with a size and depth mainly depending on the proton fluence and energy.

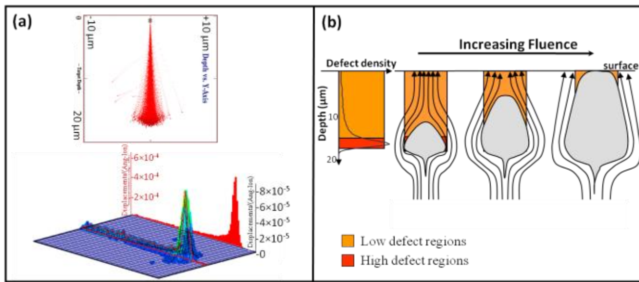

Figure 1: (a) SRIM simulation[13] of (top) trajectories versus depth and (bottom) defect distribution for 1MeV protons in silicon. (b) schematic showing the damage profile and deflected hole current around high defect region during anodization. At suitable fluences, the total hole current bends round the high defect region and flows through the lower defect region.

In this paper we describe further development of this process for micromachining of complex, 3D suspended silicon structures in 0.4 Ω.cm p-type silicon, chosen as suitable for fabricating components for silicon photonics, where as low carrier density is required to reduce propagation loss by scattering from free carriers [1]. Wafers are then electrochemically anodized in an electrolyte containing HF (48%):water:ethanol (1:1:2) for 12 minutes with a current density of 60 mA/cm^2, giving an etch depth of about 27 µm. During the electrochemical process, the flow of electrical holes from the back surface bends around the high defect regions to the front surface. As a result PSi forms around these regions, leaving the core region intact, with a size and depth depending on the proton fluence and energy.

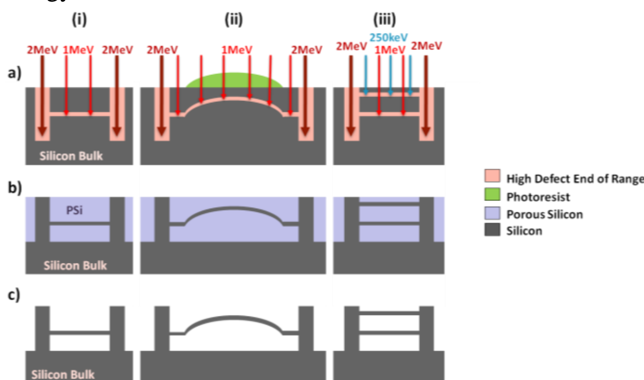

Figure 2: Schematics of the processes involved in fabricating (i) flat, (ii) curved and (iii) multilevel free standing 3D wires using (a) 1MeV and 250keV proton irradiation for wires and 2MeV protons with a high line fluence for supporting walls, (b) anodization to produce PSi around the cores and (c) removal of the PSi leaving a free-standing structure.

Schematics of the three irradiation processes used in this paper are shown in the columns (i) to (iii) in Fig. 2. Supporting walls for the final free-standing structures are defined using 2 MeV protons (range of ~48µm) with a high line fluence of 1.2×10^{12}/cm, which is enough to completely stop anodization at the irradiated regions. In process (i), single energy (1 MeV) proton irradiation with a low line fluence of 1×10^{10}/cm is used to create end-of-range cores at a single depth. Focused beam irradiation may be of any shape, such as lines or circles. During anodization in Fig. 2 (b), current flows through those regions above and below the end-of-range core region, resulting in PSi formation. No current flows through the core or the supports. Finally, very dilute KOH solution is used to release the suspended 3D silicon structures, Fig. 2 (c).

3 RESULTS AND DISCUSSIONS

The standard definition of fluence, the number of ions incident upon a given surface area in units of ions/cm^2, is ideal for irradiating large areas where the effects of irradiation are laterally uniform and the defect depth distribution may be calculated using codes such as SRIM[13]. However, for studying the unusual irradiation regime in which ion scattering results in a lateral extent of the defects across the end-of-range region is significantly larger than the irradiated line width on the wafer surface, fluence is not the most relevant factor in determining the core size. As the surface width of an irradiated line becomes similar to, or less than, the end-of-range lateral scattering, the peak defect density decreases even though the fluence remains the same. Hence, the number of ions used for irradiating a line of zero width per centimeter of line length, Ψ, is a more useful parameter. This definition is independent of any variations or uncertainty in the irradiated line width on the surface and it simplifies the experimental aspects of fabricating small cores since the only parameter is the total number of ions used, and the line length. For example, Fig. 3 shows cross-sectional optical images of cores formed silicon using PBW with 1 MeV protons and surface line width and irradiated Ψ of (a) 500 nm, 3×10^{10}/cm, (b) 1000 nm, 1×10^{10}/cm. Smaller core sizes of ~2 µm are formed with 1 MeV protons in Fig. 3 (b) because Ψ is lower than in Fig. 3 (a), even though the irradiated line width is greater.

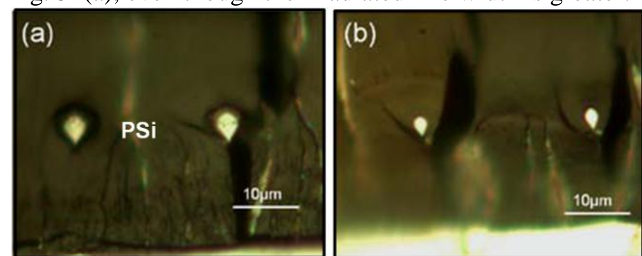

Figure 3 : Cross-section optical micrographs showing core sizes for surface line width and irradiated Ψ of 1 MeV protons of (a) 500 nm, 3×10^{10}/cm, (b) 1000 nm, 1×10^{10}/cm.

Fig. 4 shows cross-section optical images of cores produced in the same resistivity by irradiation with increasing Ψ of 1 MeV protons using PBW and a beam focused to a spot size of 200 nm. By increasing the Ψ from 1.5×10^{10}/cm to 1.2×10^{11}/cm the width of the core increases from about 1 µm to 5 µm respectively. At the same time the core cross-section elongates, as shown in Fig. 4 (b), as the

defect density all along the irradiation path increases to the level where it significantly deflects the flow of hole current. Hence smaller core size is expected at lower Ψ.

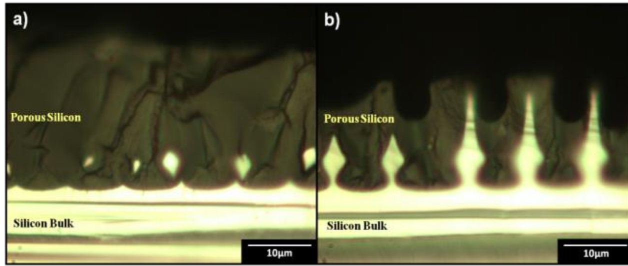

Figure 4 : Optical images showing wire cross-sections buried in PSi in 0.4 Ω.cm wafer after irradiation with 1MeV protons with a Ψ of (a) 1.5×10^{10}/cm, 3×10^{10}/cm, (b) 6×10^{10}/cm and 1.2×10^{11}/cm.

To fabricate small cores, a low proton energy seems preferable, also it requires a lower fluence to achieve a given peak defect density. This is because the decreased scattering at lower ion energies results in a smaller, denser defect distribution. An example of cores irradiated using PBW with 250 keV protons (with range of ~2.5 µm) with Ψ of 1×10^{10}/cm and 3×10^{10}/cm can be seen in Fig. 5, where for the lower fluence the core size is ~200nm. The core size can even become smaller by decreasing the irradiation energy and fluence.

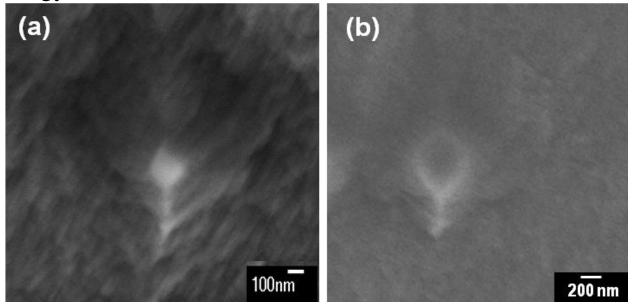

Figure 5 : Cross-section SEM images showing cores formed in 0.4 Ω.cm p-type silicon wafer irradiated with 250 keV protons using (a) Ψ=1×10^{10}/cm and (b) Ψ=3×10^{10}/cm.

Using this process, we have fabricated arrays of long wires using the approach in Fig. 2(i) by irradiating lines of 500 µm length with 1 MeV protons, Fig. 6. A long supporting wall mid-way along their length and shorter ones at different spacings were included with the aim of studying how long such suspended wires could be made. None of the wires have broken, showing that suspended wires of diameter about 1 µm can be produced over 400 µm long. The higher magnification SEMs in Fig. 6 shows the end of the wires suspended above the etched silicon surface and details of where the wire joins the support.

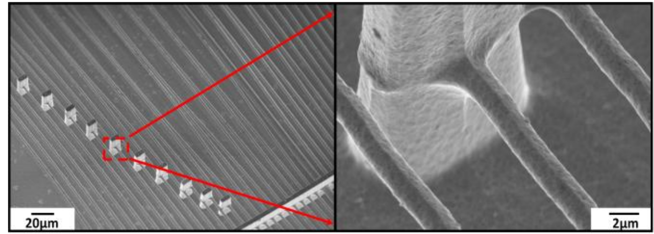

Figure 6 : SEM images of 3D machined arrays of suspendedd wires and its close-up views, supported by heavily irradiated silicon walls.

Using proton beam writing for selective irradiation gives the ability to directly fabricate arbitrary patterns, not necessarily just lines as described above. Fig. 7 (a) shows a simple suspended silicon spring suporrted by two pillars, fabricated as an example to show the further capability of this technique for fabricating more complicated structures. Fig. 7 (b) shows a grid structure, formed using the same process except using 250 keV protons (range 2.6 µm, FWHM 460 nm), line fluence of 1×10^{10}/cm to produce the end-of-range cores as a grid structure, again supported by higher energy irradiations. Since the FWHM beam spread at the end-of-range is considerably smaller than for 1 MeV protons, a smaller wire cross-section of 800 nm is produced.

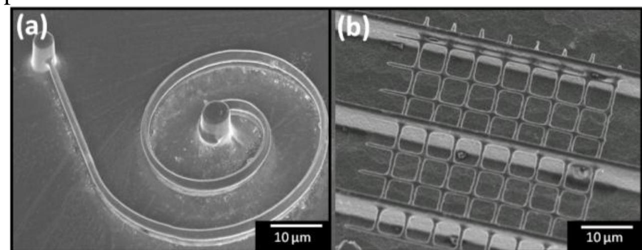

Figure 7 : Examples of process (i) of Fig. 2, (a) spring formed with 1 MeV proton irradiation and (b) grid formed by irradiation with 250 keV protons.

Micro- and nano-structures curved in the vertical plane can be similarly micromachined, with the addition of a thin, patterned gray-scale resist mask with tapered edges, figure 2 process (ii). The resist is thin enough so protons can penetrate the underlying silicon. Because of the resist thickness, the proton end-of-range depth in the silicon is modified according to the resist profile. Such spatial variations of the end-of-range enable 3D silicon microstructures which are curved in the vertical direction, Fig.8 (a),(b).

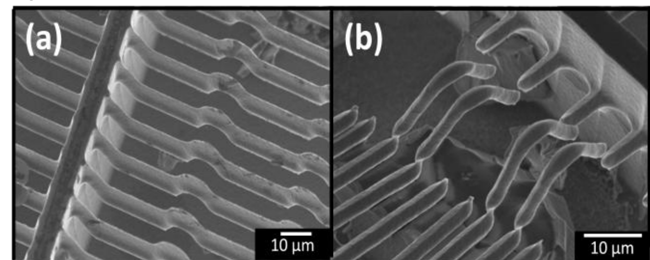

Figure 8 : Examples of process (ii) of Fig. 2, curved 3D fabrication using 1 MeV protons.

NSTI-Nanotech 2013, www.nsti.org, ISBN 978-1-4822-0584-8 Vol. 2, 2013

Multiple energy proton irradiation can be used to create localized defects at different depths within the silicon wafer to fabricate multilevel 3D structures, see process (iii) in Fig. 2. After anodization the high defect core regions, produced by different proton energies, remain intact while the surrounding low defect regions between the cores form PSi.

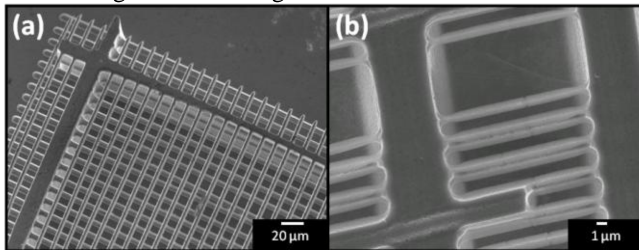

Figure 9 : Examples of process (iii) of Fig. 2, fabricated two-level array of (a) prepandcular , (b) parralel suspended wires.

An array of two-level silicon wires running in orthogonal directions was fabricated with a period of 10 µm, Fig. 9 (a). Line irradiations using 250keV protons with line fluences of 1×10^{10}/cm were used to fabricate shallow wires, while orthogonal line irradiations using 1 MeV protons with line fluences of 1×10^{10}/cm were used to fabricate deeper wires. Supporting walls were formed by irradiation using a 2 MeV proton line fluence of 1.2×10^{12}/cm. After anodization and PSi removal, orthogonal suspendded wires at different depths were revealed, Fig. 9 (b).

4 CONCLUSION

In conclusion, we demonstrate the ability of using localized defects created at the end-of-range of high energy protons for machining complex 3D silicon structures within the bulk silicon after subsequent anodization and removing the PSi process. Curved 3D multilevel silicon structures may be fabricated using a gray scale mask and multiple energy exposure. This is the only technique capable of doing so after a single step etching. We believe this process is an important development in fields such as silicon photonics and MEMS.

REFERENCES

1. G. T. Reed and A. P. Knights, Wiley (2004).
2. A. Liu, R. Jones, L. Liao, D. Samara-Rubio, D. Rubin, O. Cohen, R. Nicolaescu and M. Paniccia, Nature **427** (6975), 615-618 (2004).
3. H. Rong, R. Jones, A. Liu, O. Cohen, D. Hak, A. Fang and M. Paniccia, Nature **433** (7027), 725-728 (2005).
4. V. R. Almeida, C. A. Barrios, R. R. Panepucci and M. Lipson, Nature **431** (7012), 1081-1084 (2004).
5. A. N. Cleland and M. L. Roukes, *Fabrication of high frequency nanometer scale mechanical resonators from bulk Si crystals*. (AIP, 1996).
6. J. Fritz, M. K. Baller, H. P. Lang, H. Rothuizen, P. Vettiger, E. Meyer, H. -J. Güntherodt, C. Gerber and J. K. Gimzewski, Science **288** (5464), 316-318 (2000).
7. H. G. Craighead, Science **290** (5496), 1532-1535 (2000).
8. S. Y. Lin, J. G. Fleming, D. L. Hetherington, B. K. Smith, R. Biswas, K. M. Ho, M. M. Sigalas, W. Zubrzycki, S. R. Kurtz and J. Bur, Nature **394** (6690), 251-253 (1998).
9. S. Azimi, J. Song, Z. Y. Dang, H. D. Liang and M. B. H. Breese, Journal of Micromechanics and Microengineering **22** (11), 113001 (2012).
10. S. Azimi, M. B. H. Breese, Z. Y. Dang, Y. Yan, Y. S. Ow and A. A. Bettiol, Journal of Micromechanics and Microengineering **22** (1), 015015 (2012).
11. M. B. H. Breese, D. N. Jamieson and P. J. C. King, Wiley (1996).
12. S. Azimi, Y. S. Ow and M. B. H. Breese, Electrochemical and Solid-State Letters **13** (11), H382-H384 (2010).
13. J. F. Ziegler, M. D. Ziegler and J. P. Biersack, Nuclear Instruments and Methods in Physics Research Section B: Beam Interactions with Materials and Atoms **268** (11–12), 1818-1823 (2010).
14. M. B. H. Breese, F. J. T. Champeaux, E. J. Teo, A. A. Bettiol and D. J. Blackwood, Physical Review B **73** (3), 035428 (2006).